

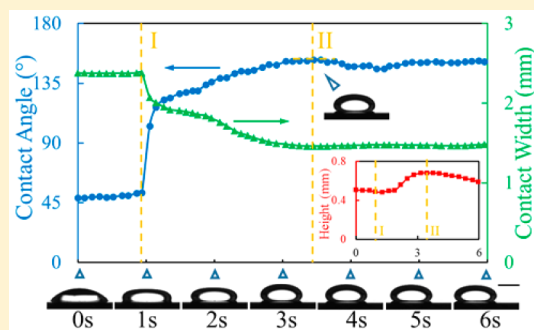
Effects of Electropolymerization Parameters of PPy(DBS) Surfaces on the Droplet Flattening Behaviors During Redox

Jian Xu, Anthony Palumbo, Wei Xu, and Eui-Hyeok Yang*

Department of Mechanical Engineering, Stevens Institute of Technology, 1 Castle Point Terrace, Hoboken, New Jersey 07030, United States

Supporting Information

ABSTRACT: We present a systematic study on the effects of electropolymerization parameters of polypyrrole-dodecylbenzenesulfonate (PPy(DBS)) surfaces on the flattening behaviors of organic droplets during reduction and oxidation (redox). PPy(DBS) surfaces were fabricated under varying electropolymerization conditions, including voltage, surface charge density, and dopant electrolyte (DBS⁻) concentration. The flattening behaviors on different PPy(DBS) surfaces were characterized by analyzing droplet behaviors and energy-dispersive X-ray spectroscopy (EDS) data. The surface charge density and voltage during electropolymerization determined the thickness and doping ratio of synthesized PPy(DBS) surfaces, affecting how DBS⁻ molecules are released from PPy(DBS) upon reduction. The release amount and rate of DBS⁻ molecules were strongly related to the droplet flattening time.



INTRODUCTION

Conjugated polymers have gained attention in several applications including actuators,¹ supercapacitors,² solar cells,³ biosensors,⁴ and microfluidics.⁵ Among various conjugated polymers, polypyrrole (PPy) has been an attractive candidate, in contribution to its good stability and biocompatibility.^{6–8} By doping with aromatic, amphiphilic, and bulky anions like dodecylbenzenesulfonate (DBS⁻), PPy can attain higher conductivity^{9,10} and improved mechanical or device properties.^{11–15} Polypyrrole-dodecylbenzenesulfonate (PPy(DBS)) can be synthesized via electropolymerization in aqueous solution of pyrrole monomer and sodium dodecylbenzenesulfonate (NaDBS). Its surface properties^{16,17} can be modified by applying low electrochemical potentials ($\sim \pm 1$ V¹), enabling applications such as underwater actuators, micropumps, and drug delivery systems.^{18–20}

Of particular interest, PPy(DBS) surfaces have demonstrated merit toward manipulating liquid droplets through the switch of wetting properties, which is related to tunable surface structure,²¹ electrical double layer,²² or reorientation and release of DBS⁻ molecules.^{23–28} Recently, the authors' group demonstrated an *in situ* control of flattening of organic droplets, and consequently, tunable adhesion on PPy(DBS) surfaces in an aqueous environment, which potentially impacts several future applications including lab-on-chip technologies, water treatments, and oil–water separation.²⁹ Results showed that the droplet flattening was caused by the decreased interfacial tension of a droplet with the surrounding medium due to the release of DBS⁻ molecules from PPy(DBS) during the reduction of the polymer. However, the relationship between the droplet flattening behaviors and the fabrication parameters

of PPy(DBS) surfaces is currently less studied or understood. These studies, therefore, warrant further exploitation on varying fabrication parameters such as voltage, surface charge density, and DBS⁻ concentration.

Here, we present a systematic study concerning the effects of electropolymerization parameters of PPy(DBS) surfaces on the flattening behaviors of organic droplets on these surfaces during redox in an aqueous environment. We synthesize various PPy(DBS) surfaces via varying electropolymerization voltage, surface charge density, and DBS⁻ concentration. We then characterize droplet flattening behaviors in relation to the effects of the release of DBS⁻ molecules on droplet flattening.

MATERIAL AND METHODS

Fabrication of PPy(DBS) Surfaces. PPy(DBS) surfaces were fabricated via electropolymerization, using substrates fabricated by depositing a 10 nm layer of chromium (Cr), followed by a 30 nm layer of gold (Au), on silicon wafers via e-beam evaporator (Explorer 14, Denton Vacuum, Moorestown, NJ, USA). During electropolymerization, each substrate (1 × 1 cm) was submerged as the working electrode in a solution consisting of 1 mL pyrrole (reagent grade, 98%, Sigma-Aldrich, St. Louis, MO, USA) and 150 mL NaDBS with a concentration of either 0.1 or 0.01 M (technical grade, Sigma-Aldrich, St. Louis, MO, USA). A saturated calomel electrode (SCE) and a 5 × 5 cm Cr/Au coated silicon substrate were also submerged in the solution as the reference electrode and the counter

Received: June 6, 2016

Revised: August 12, 2016

electrode, respectively. PPy(DBS) surfaces were synthesized by applying constant potentials (0.5, 0.6, 0.7, and 0.8 V versus SCE) to the working electrode until the desired surface charge density was achieved (50, 100, 200, and 300 mC/cm²). The time required to fabricate PPy(DBS) surfaces with different combinations of fabrication parameters is shown in Figure S1 (Supporting Information). The thicknesses of PPy(DBS) surfaces synthesized with different fabrication parameters were also measured using a scanning electron microscope (Auriga Small Dual-Beam FIB-SEM, Carl Zeiss, Jena, Germany).

Setup for Droplet Actuation. The experimental setup for droplet flattening is shown in Figure S2. To compare the flattening behaviors on different PPy(DBS) surfaces, dichloromethane (DCM) ($\geq 99.8\%$, Sigma-Aldrich, St. Louis, MO, USA) droplets ($\sim 1.5 \mu\text{L}$) were placed on oxidized PPy(DBS) surfaces, and their behaviors upon surface reduction were recorded and analyzed using a goniometer system (Model 250, Ramé-hart, Netcong, NJ, USA). Twenty five milliliters of freshly made 0.1 M sodium nitrate (NaNO_3 , $\geq 99.0\%$, Sigma-Aldrich, St. Louis, MO, USA) was used as the aqueous electrolyte. A 13×35 mm platinum (Pt) mesh and an SCE were used as the counter electrode and reference electrode, respectively. Oxidation and reduction of PPy(DBS) surfaces were conducted at +0.6 V and -0.9 V vs SCE, respectively.

Energy-Dispersive X-ray Spectroscopy (EDS) Measurements. EDS measurements were performed on PPy(DBS) surfaces fabricated using different electropolymerization parameters to study the loss of DBS^- molecules during redox cycles. These PPy(DBS) surfaces were analyzed using an EDS system (Model X-Max 80 mm², Oxford Instruments, Abingdon, UK), configured to a scanning electron microscope (Auriga Small Dual-Beam FIB-SEM, Carl Zeiss, Jena, Germany), after 0, 1, 2, 5, 10, 20, 50, or 100 redox cycles. Each redox cycle consisted of 1, 2, 3, 5, 7, 9, 11, 13, or 15s of reduction and 2 or 15s of oxidation.

RESULTS AND DISCUSSION

Droplet Flattening. Figure 1 shows the typical flattening behavior of a DCM droplet on a PPy(DBS) surface during reduction in an aqueous electrolyte environment (0.1 M

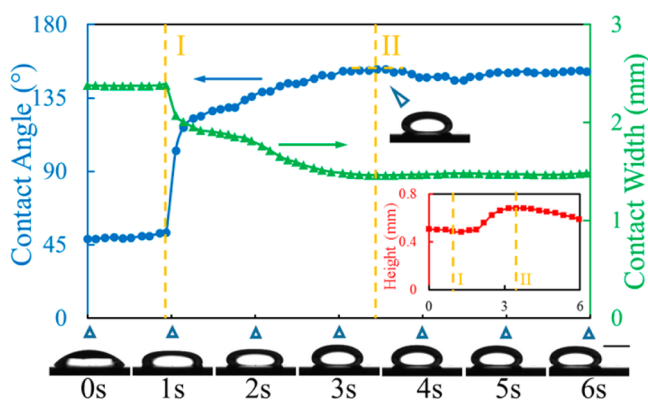


Figure 1. Flattening behavior of a DCM droplet on a PPy(DBS) surface during the reduction. Change of contact angle, contact width, and height of the droplet during the reduction of PPy(DBS) at -0.9 V. The PPy(DBS) surface was fabricated with a voltage of 0.8 V, surface charge density of 200 mC/cm², and 0.1 M NaDBS solution. Scale bar = 1 mm.

NaNO_3 solution). The droplet changed from a spherical to elliptical shape (i.e., flattening) after approximately 1 s of reduction (labeled 'I'). From 1 s to 2 s, the contact width of the droplet decreased by 25% (from 2.4 mm to 1.8 mm), and the contact angle increased from 52.5° to 136.0° . In addition, the height of the DCM droplet increased due to the droplet's constant volume. After approximately 3.5 s of reduction (labeled "II"), the contact angle, contact width, and height of DCM droplet each reached a plateau (the slight decrease of height was due to the droplet rolling out of the goniometer's focus), indicating the completion of droplet flattening.

Figure 2 illustrates the mechanism of droplet flattening, and detailed analysis on the mechanism of droplet flattening has

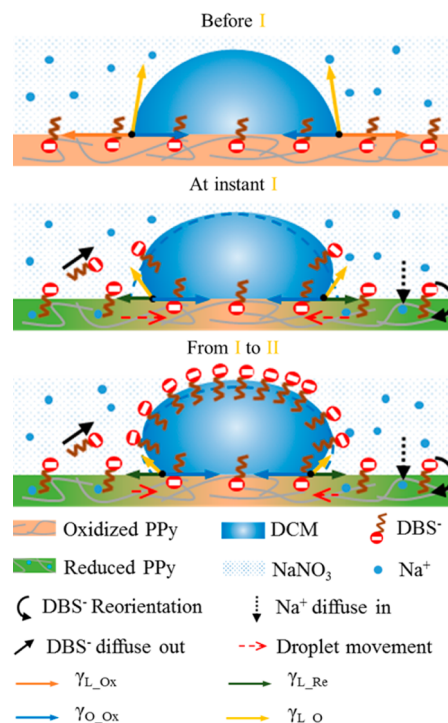


Figure 2. Mechanism of the flattening of a DCM droplet on a PPy(DBS) surface undergoing reduction, involving the reorientation of DBS^- molecules, outward diffusion (release) of DBS^- molecules, and inward diffusion (ion neutralization) of Na^+ ions.²⁵

been reported elsewhere.²⁹ In oxidized PPy(DBS), the DBS^- molecules bond to PPy chains with sulfonic acid groups, leaving hydrophobic (oleophilic) dodecyl chains to protrude out from the surface.²⁵ This makes oxidized PPy(DBS) surfaces relatively more oleophilic, and the DCM droplet stationed on the surface has a contact angle of 48.8° (0 s in Figure 1). Upon reduction, the PPy(DBS) surface exposed to the aqueous electrolyte is reduced and absorbs Na^+ cations from the electrolyte for charge neutralization.^{1,25} However, since the DCM droplet is immiscible in water, it acts as a barrier between the electrolyte and the PPy(DBS) surface in contact with the droplet. Therefore, the PPy(DBS) surface directly underneath the DCM droplet remains oxidized due to the lack of accessibility to cations. The DBS^- molecules in the reduced PPy(DBS) no longer bond to the PPy backbones, but they reorient within the PPy(DBS) and expose the hydrophilic (or oleophobic) sulfonic acid groups at the outermost surface, which makes the reduced polymer surface more oleophobic. Thus, the contact angle increased dramatically from 48.8° to 152.7° (Figure 1 inset).

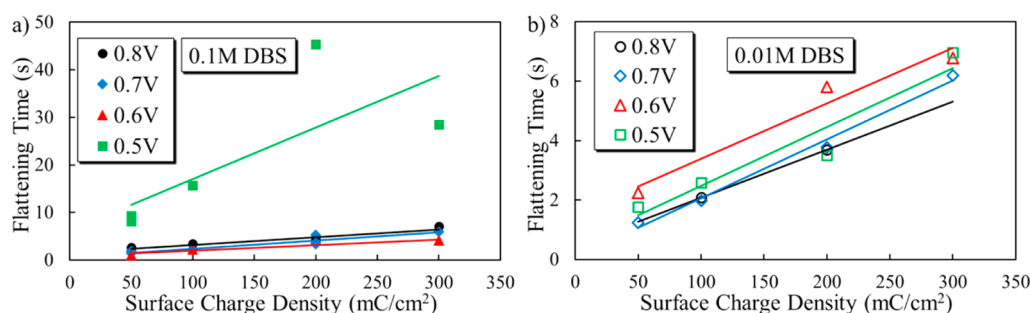


Figure 3. Flattening times of DCM droplets on PPy(DBS) surfaces, fabricated using (a) 0.1 M NaDBS and (b) 0.01 M NaDBS.

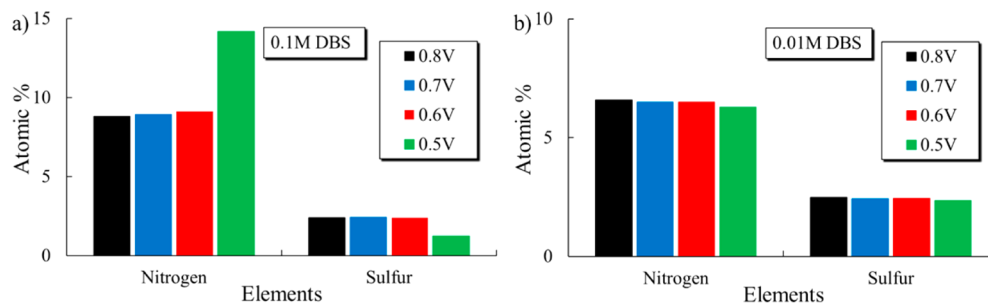


Figure 4. Atomic % of nitrogen and sulfur elements of PPy(DBS) surfaces fabricated using (a) 0.1 M NaDBS and (b) 0.01 M NaDBS.

The surface tension between the aqueous solution and the PPy(DBS) surface changes from $\gamma_{L_{Ox}}$ (surface tension between aqueous solution and oxidized PPy(DBS) surface) to $\gamma_{L_{Re}}$ (surface tension between aqueous solution and reduced PPy(DBS) surface). Since $\gamma_{L_{Re}}$ is smaller than $\gamma_{L_{Ox}}$,²⁵ the lateral interfacial tensions at the droplet contact line are no longer balanced, causing the contact line to move inward. Furthermore, a minute amount of DBS⁻ molecules escapes from the PPy chains, indicated by the decrease of the sulfur (S) to carbon (C) ratio of the PPy(DBS) surface (detailed discussion is in the “Surface Charge Density and Rate of DBS⁻ Molecules Release” section and has been reported elsewhere²⁹). The released DBS⁻ molecules accumulate at the DCM droplet-aqueous electrolyte interface and significantly decrease the interfacial tension ($\gamma_{L_{O}}$) as a result. Consequently, the DCM droplet cannot maintain the shape by interfacial tension and flattens due to the effect of gravity.²⁹

PPy(DBS) surfaces fabricated under different conditions, including voltage, surface charge density, and DBS⁻ concentration, were tested in order to investigate the effects of fabrication parameters on DCM droplet flattening time (the time required for the completion of droplet flattening). As shown in Figure 3, given the same fabrication voltage (0.5, 0.6, 0.7, and 0.8 V) and NaDBS solution concentration (0.1 and 0.01 M), the flattening time, characterized by maximal contact angle, maximal height, and minimal contact width of droplets, exhibited a positive linear relationship with surface charge density. When using 0.1 M NaDBS solution (Figure 3a), the droplet flattening times on PPy(DBS) surfaces fabricated at 0.6–0.8 V were similar and increased from ~1.8 to ~5.8 s when the surface charge density increased from 50 to 300 mC/cm². Compared to the PPy(DBS) surfaces fabricated between 0.6 and 0.8 V, surfaces fabricated at 0.5 V showed particularly longer and less consistent flattening, which is discussed in the next section. When using 0.01 M NaDBS solution (Figure 3b), the droplet flattening time on PPy(DBS) surfaces fabricated at 0.5–0.8 V increased from ~1.8 to ~6.7 s when the surface

charge density increased from 50 to 300 mC/cm². Therefore, a PPy(DBS) surface fabricated with a higher surface charge density resulted in a longer DCM droplet flattening time during reduction (regardless of fabrication voltage or NaDBS solution concentration).

Fabrication Voltage and PPy(DBS) Doping Ratio. The EDS data (Figure 4) shows the elemental composition of PPy(DBS) fabricated under different conditions. Results showed that the PPy(DBS) fabricated at 0.5 V and with 0.1 M NaDBS had a much lower percentage of sulfur (1.2%), compared to those fabricated at higher voltages (nearly consistent at 2.4%), as is also observed for PPy(DBS) fabricated with 0.01 M NaDBS. Meanwhile, PPy(DBS) fabricated at 0.5 V and 0.1 M NaDBS had a much higher percentage of nitrogen. Since nitrogen only exists in PPy chains and sulfur only exists in DBS⁻ dopants, their ratio indicates the “doping ratio” (the ratio of DBS⁻ molecules to pyrrole monomers). Thus, PPy(DBS) fabricated using 0.5 V and 0.1 M NaDBS had a significantly lower doping ratio than the case of PPy(DBS) fabricated at higher voltages. It is known that the typical doping ratio for electropolymerized PPy(DBS) is between 1/3 and 1/4.¹ However, the doping ratio for PPy(DBS) fabricated at 0.5 V in 0.1 M NaDBS was around 1/12, according to the ratio between sulfur and nitrogen, acquired through EDS measurements. Therefore, PPy(DBS) fabricated at 0.5 V and 0.1 M NaDBS had a lower amount of DBS⁻ dopants. The decreased proportion of DBS⁻ molecules in PPy(DBS) fabricated using 0.5 V and 0.1 M NaDBS may result in a much smaller amount of DBS⁻ molecules released from PPy(DBS) to facilitate flattening, which explains the significantly slower droplet flattening on the surfaces during reduction.

Surface Charge Density and Rate of DBS⁻ Molecules Release. Since the flattening of droplets is related to the release of DBS⁻ molecules from PPy(DBS), we investigated the effect of fabrication parameters on the release of DBS⁻ molecules via EDS, through the change of elemental composition of PPy(DBS) during redox cycles. The ratio of

sulfur to carbon (S/C) was used to indicate the amount of DBS⁻ molecules remaining in the PPy(DBS) surfaces, since sulfur atoms only exist in DBS⁻ molecules. As shown in Figure 5, among PPy(DBS) surfaces fabricated using 0.6–0.8 V and

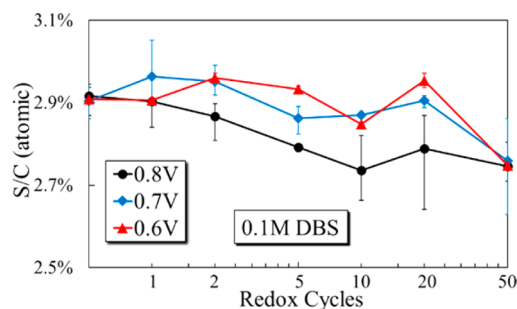


Figure 5. S/C ratio of PPy(DBS) surfaces fabricated with different voltages after 50 redox cycles. Each redox cycle consisted of 15 s of reduction and 15 s of oxidation. The PPy(DBS) surfaces were each fabricated with a surface charge density of 300 mC/cm² and NaDBS solution concentration of 0.1 M.

0.1 M NaDBS, there was no significant difference observed for the change of S/C ratio during 50 redox cycles, which agrees with the similar flattening times on those samples.

However, the surface charge density used for the fabrication of PPy(DBS) surfaces was found to strongly affect the rate of release of DBS⁻ molecules during redox. As shown in Figure 6a, PPy(DBS) fabricated at a higher surface charge density experienced a smaller decrease in S/C ratio over successive redox cycles, consisting of 2 s of reduction and 2 s of oxidation. The PPy(DBS) surface fabricated at 50 mC/cm² experienced a 7.9% decrease of S/C, compared with only a 1.9% decrease for PPy(DBS) fabricated at 300 mC/cm², after 100 redox cycles. Once the redox cycles consisted of 15 s of reduction and 15 s of oxidation, the difference in the amount of S/C decrease

continued to persist (Figure 6b). Figure 6c shows S/C data of PPy(DBS) surfaces after 20 redox cycles consisting of varying reduction durations and 15 s of oxidation. While there was no significant change in S/C for PPy(DBS) surfaces fabricated at 300 mC/cm², PPy(DBS) fabricated at 50 mC/cm² experienced an 18.5% decrease of S/C, and the most significant decrease occurred when the reduction time in each cycle was shorter than 3 s. After 100 cycles (Figure 6d), PPy(DBS) surfaces fabricated at 300 mC/cm² experienced a 19.2% decrease of S/C, and no significant decrease was observed until the reduction time in each cycle was longer than 11 s. These results indicate that a PPy(DBS) surface fabricated with a higher surface charge density released DBS⁻ molecules slower, and the released amount was also smaller during reduction when compared to a PPy(DBS) surface fabricated with a lower surface charge density.

We have also found that the thickness of the PPy(DBS) film increased with the surface charge density. As shown in Figure 7a, if fabricated using 0.1 M NaDBS and 0.6–0.8 V, the thickness of the PPy(DBS) film linearly increased from ~254 nm to ~1592 nm when the surface charge density increased from 50 to 300 mC/cm². If fabricated using 0.01 M NaDBS, the thickness of the PPy(DBS) surface similarly increased from ~212 nm to ~1054 nm when the surface charge density increased from 50 to 300 mC/cm² (Figure 7b). These results demonstrate that PPy(DBS) surfaces with higher thicknesses release DBS⁻ molecules slower than thinner surfaces. We deduce that thicker PPy(DBS) surfaces fabricated with higher surface charge densities require longer times for DBS⁻ molecules to be released during reduction, thus increasing the flattening times of DCM droplets.

CONCLUSION

We have studied the effects of electropolymerization parameters on the flattening behavior of organic droplets on

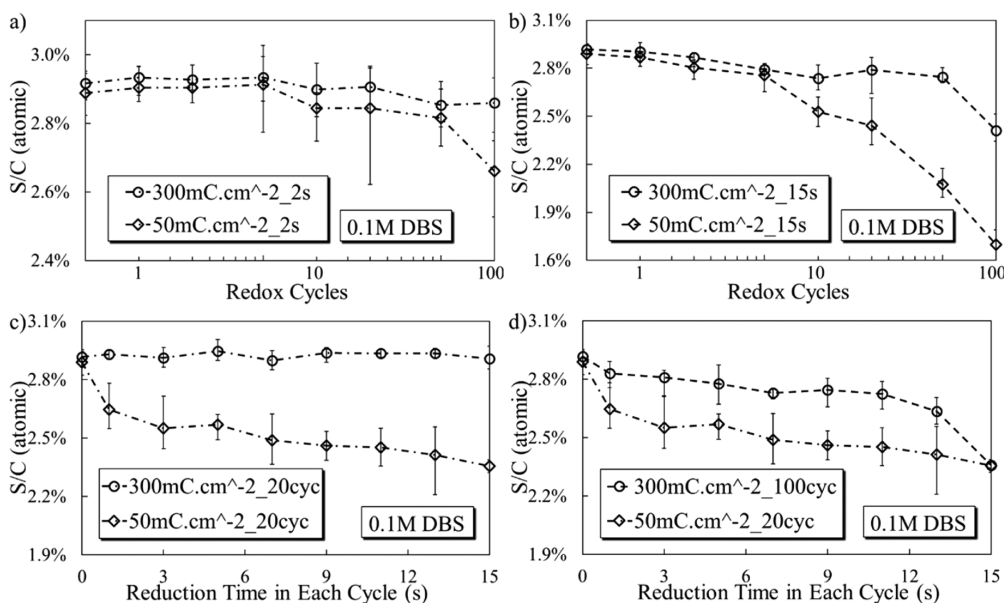


Figure 6. Change of sulfur/carbon (S/C) ratio of PPy(DBS) surfaces fabricated at surface charge densities of 50 mC/cm² and 300 mC/cm² (0.1 M NaDBS solution, 0.8 V) during redox cycles consisting of (a) 2 s of reduction and 2 s of oxidation or (b) 15 s of reduction and 15 s of oxidation. (c) Change of S/C ratio of PPy(DBS) surfaces after 20 redox cycles consisting of varying reduction durations from 1 to 15 s and oxidation of 15 s. (d) Comparison of S/C ratio of PPy(DBS) surfaces fabricated with 50 mC/cm² after 20 redox cycles to a PPy(DBS) surface of 300 mC/cm² after 100 redox cycles.

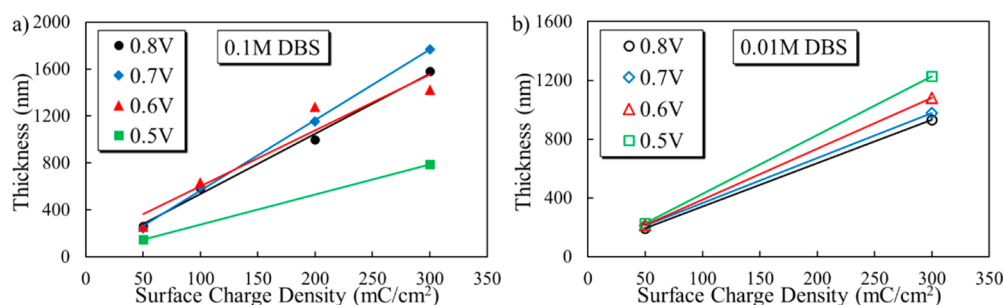


Figure 7. Thicknesses of PPy(DBS) surfaces fabricated with NaDBS solution concentration of (a) 0.1 M and (b) 0.01 M.

PPy(DBS) surfaces upon redox. We have fabricated different PPy(DBS) surfaces by varying fabrication parameters, including voltage, surface charge density, and NaDBS electrolyte concentration. The thickness of a PPy(DBS) film, determined by surface charge density during electropolymerization, was found to strongly affect the release of DBS⁻ molecules from the PPy(DBS) surface, confirmed by EDS characterization. We have found that thinner PPy(DBS) films (fabricated with lower surface charge densities, given the fabrication voltage is high enough for proper electropolymerization) lose DBS⁻ molecules quicker during reduction, which results in a faster droplet flattening. This work gives rise to the possibility of tailoring the droplet actuation behaviors on polymer surfaces by adjusting the parameters of electropolymerization.

■ ASSOCIATED CONTENT

● Supporting Information

The Supporting Information is available free of charge on the ACS Publications website at DOI: 10.1021/acs.jpcc.6b05698.

Fabrication time of different PPy(DBS) surfaces and experiment setup for droplet flattening test (PDF)

■ AUTHOR INFORMATION

Corresponding Author

*E-mail: eyang@stevens.edu; Telephone: +1 (201) 216-5574; Fax: +1 (201) 216-8315.

Notes

The authors declare no competing financial interest.

■ ACKNOWLEDGMENTS

This work has been supported in part by National Science Foundation award (ECCS-1202269). This work has also been partially carried out at the Micro Device Laboratory (MDL) funded with support from Contract# W15QKN-05-D-0011 and the Laboratory for Multiscale Imaging (LMSI) partially funded by the National Science Foundation (DMR-0922522) at Stevens Institute of Technology.

■ REFERENCES

- (1) Smela, E. Microfabrication of PPy Microactuators and Other Conjugated Polymer Devices. *J. Micromech. Microeng.* **1999**, *9*, 1–18.
- (2) Shi, Y.; Pan, L.; Liu, B.; Wang, Y.; Cui, Y.; Bao, Z.; Yu, G. Nanostructured Conductive Polypyrrole Hydrogels as High-Performance, Flexible Supercapacitor Electrodes. *J. Mater. Chem. A* **2014**, *2*, 6086.
- (3) Jeong, S.; Garnett, E. C.; Wang, S.; Yu, Z.; Fan, S.; Brongersma, M. L.; McGehee, M. D.; Cui, Y. Hybrid Silicon Nanocone-Polymer Solar Cells. *Nano Lett.* **2012**, *12*, 2971–2976.
- (4) Ates, M. A Review Study of (Bio)sensor Systems Based on Conducting Polymers. *Mater. Sci. Eng., C* **2013**, *33*, 1853–1859.
- (5) Chang, J. H.; Hunter, I. W. A Superhydrophobic to Superhydrophilic in Situ Wettability Switch of Microstructured Polypyrrole Surfaces. *Macromol. Rapid Commun.* **2011**, *32*, 718–723.
- (6) Skotheim, T. A.; Reynolds, J. R. *Handbook of Conducting Polymers*; CRC Press, 2007; Vol. 2.
- (7) Zha, Z.; Deng, Z.; Li, Y.; Li, C.; Wang, J.; Wang, S.; Qu, E.; Dai, Z. Biocompatible Polypyrrole Nanoparticles as a Novel Organic Photoacoustic Contrast Agent for Deep Tissue Imaging. *Nanoscale* **2013**, *5*, 4462–4467.
- (8) George, P. M.; Lyckman, A. W.; LaVan, D. A.; Hegde, A.; Leung, Y.; Avasare, R.; Testa, C.; Alexander, P. M.; Langer, R.; Sur, M. Fabrication and Biocompatibility of Polypyrrole Implants Suitable for Neural Prosthetics. *Biomaterials* **2005**, *26*, 3511–3519.
- (9) An, H.; Haga, Y.; Yuguchi, T.; Yosomiya, R. Synthesis of Polypyrrole by Electrochemical Polymerization Using Organic Anion Electrolytes and Its Application. *Angew. Makromol. Chem.* **1994**, *218*, 137–151.
- (10) Kupila, E.-L.; Kankare, J. Electropolymerization of Pyrrole: Effects of pH and Anions on the Conductivity and Growth Kinetics of Polypyrrole. *Synth. Met.* **1993**, *55*, 1402–1405.
- (11) Naoi, K.; Lien, M.; Smyrl, W. H. Quartz Crystal Microbalance Study: Ionic Motion across Conducting Polymers. *J. Electrochem. Soc.* **1991**, *138*, 440–445.
- (12) Pei, Q.; Inganäs, O. Electrochemical Applications of the Bending Beam Method. 2. Electroshrinking and Slow Relaxation in Polypyrrole. *J. Phys. Chem.* **1993**, *97*, 6034–6041.
- (13) Gandhi, M. R.; Murray, P.; Spinks, G. M.; Wallace, G. G. Mechanism of Electromechanical Actuation in Polypyrrole. *Synth. Met.* **1995**, *73*, 247–256.
- (14) Bhattacharya, A.; De, A.; Das, S. Electrochemical Preparation and Study of Transport Properties of Polypyrrole Doped with Unsaturated Organic Sulfonates. *Polymer* **1996**, *37*, 4375–4382.
- (15) Naoi, K.; Oura, Y.; Maeda, M.; Nakamura, S. Electrochemistry of Surfactant-Doped Polypyrrole film(I): Formation of Columnar Structure by Electropolymerization. *J. Electrochem. Soc.* **1995**, *142*, 417–422.
- (16) Wang, X.; Smela, E. Color and Volume Change in PPy(DBS). *J. Phys. Chem. C* **2009**, *113*, 359–368.
- (17) Wang, X.; Smela, E. Experimental Studies of Ion Transport in PPy(DBS). *J. Phys. Chem. C* **2009**, *113*, 369–381.
- (18) Naka, Y.; Fuchiwaki, M.; Tanaka, K. A Micropump Driven by a Polypyrrole-Based Conducting Polymer Soft Actuator. *Polym. Int.* **2010**, *59*, 352–356.
- (19) Xu, H.; Wang, C.; Wang, C.; Zoval, J.; Madou, M. Polymer Actuator Valves toward Controlled Drug Delivery Application. *Biosens. Bioelectron.* **2006**, *21*, 2094–2099.
- (20) Chatzipiridis, G.; Sanoria, A.; Ergeneman, O.; Sort, J.; Puigmartí-Luis, J.; Nelson, B. J.; Pellicer, E.; Pané, S. The Electrochemical Manipulation of Apolar Solvent Drops in Aqueous Electrolytes by Altering the Surface Polarity of Polypyrrole Architectures. *Electrochem. Commun.* **2015**, *54*, 32–35.
- (21) Liu, M.; Nie, F.-Q.; Wei, Z.; Song, Y.; Jiang, L. In Situ Electrochemical Switching of Wetting State of Oil Droplet on Conducting Polymer Films. *Langmuir* **2010**, *26*, 3993–3997.

(22) Liu, M.; Liu, X.; Ding, C.; Wei, Z.; Zhu, Y.; Jiang, L. Reversible Underwater Switching between Superoleophobicity and Superoleophilicity on Conducting Polymer Nanotube Arrays. *Soft Matter* **2011**, *7*, 4163.

(23) Halldorsson, J. A.; Wu, Y.; Brown, H. R.; Spinks, G. M.; Wallace, G. G. Surfactant-Controlled Shape Change of Organic Droplets Using Polypyrrole. *Thin Solid Films* **2011**, *519*, 6486–6491.

(24) Halldorsson, J. A.; Little, S. J.; Diamond, D.; Spinks, G. M.; Wallace, G. G. Controlled Transport of Droplets Using Conducting Polymers. *Langmuir* **2009**, *25*, 11137–11141.

(25) Tsai, Y.-T.; Choi, C.-H.; Gao, N.; Yang, E. H. Tunable Wetting Mechanism of Polypyrrole Surfaces and Low-Voltage Droplet Manipulation via Redox. *Langmuir* **2011**, *27*, 4249–4256.

(26) Tsai, Y.-T.; Choi, C.-H.; Yang, E. H. Low-Voltage Manipulation of an Aqueous Droplet in a Microchannel via Tunable Wetting on PPy(DBS). *Lab Chip* **2013**, *13*, 302–309.

(27) Xu, W.; Tian, Y.; Bisaria, H.; Ahn, P.; Choi, C.-H.; Yang, E. H. Transportation of a Liquid Droplet at Ultra-Low Voltages by Tunable Wetting on Conjugated Polymer Electrodes. In *IEEE International Conference on Solid-State Sensors, Actuators and Microsystems (Transducers '13)*; 2013; pp 2185–2188.

(28) Xu, W.; Li, X.; Palumbo, A.; Choi, C.-H.; Yang, E. H. Bi-Directional Switching of Microdroplet Adhesion on Doped Polypyrrole Microstructures. In *Hilton Head Workshop 2014: A Solid-State Sensors, Actuators & Microsystems Workshop*; 2014.

(29) Xu, W.; Xu, J.; Choi, C.-H.; Yang, E. H. In Situ Control of Underwater-Pinning of Organic Droplets on a Surfactant-Doped Conjugated Polymer Surface. *ACS Appl. Mater. Interfaces* **2015**, *7*, 25608–25617.